

- Copyright permission to reproduce figures and/or text from this article

[View the Full Text HTML](#)



Design, Synthesis, and Computational Studies of Inhibitors of Bcl-X_L

Cheol-Min Park,^{*,†} Tetsuro Oie,[‡] Andrew M. Petros,[‡] Haichao Zhang,[†]
Paul M. Nimmer,[†] Rodger F. Henry,[‡] and Steven W. Elmore[†]

Contribution from Global Pharmaceutical R&D, Abbott Laboratories, 100 Abbott Park Road,
Abbott Park, Illinois 60064

Received July 14, 2006; E-mail: cheol-min.park@abbott.com

Abstract: One of the primary objectives in the design of protein inhibitors is to shape the three-dimensional structures of small molecules to be complementary to the binding site of a target protein. In the course of our efforts to discover potent inhibitors of Bcl-2 family proteins, we found a unique folded conformation adopted by tethered aromatic groups in the ligand that significantly enhanced binding affinity to Bcl-X_L. This finding led us to design compounds that were biased by nonbonding interactions present in a urea tether to adopt this bioactive, folded motif. To characterize the key interactions that induce the desired conformational bias, a series of substituted *N,N*-diarylureas were prepared and analyzed using X-ray crystallography and quantum mechanical calculations. Stabilizing π -stacking interactions and destabilizing steric interactions were predicted to work in concert in two of the substitution patterns to promote the bioactive conformation as a global energy minimum and result in a high target binding affinity. Conversely, intramolecular hydrogen bonding present in the third substitution motif promotes a less active, extended conformer as the energetically favored geometry. These findings were corroborated when the inhibition constant of binding to Bcl-X_L was determined for fully elaborated analogues bearing these structural motifs. Finally, we obtained the NMR solution structure of the disubstituted *N,N*-diarylurea bound to Bcl-X_L demonstrating the folded conformation of the urea motif engaged in extensive π -interactions with the protein.

Introduction

In recent years, the manipulation of conformations of flexible molecules has attracted great interest.^{1–3} The ability to achieve specific conformations for proteins and small organic molecules is crucial for their chemical and biological functions. A number of bioactive natural products with conformational flexibility rely upon specific conformations to present functional groups in specific orientations for their activity, and for optimal binding, the functional groups should be complementary to those in the protein binding site.⁴ The concept of preorganization has been widely utilized in many areas, including molecular recognition and drug design.^{5–7} Constraining flexible ligands by covalent bonds in such a way that they represent bound conformations may benefit from an entropic factor.^{8–13} However, the difficulty to precisely mimic the bound conformation by covalent modi-

fication often results in the loss of enthalpic energy that can offset the gain in the entropic term.^{14–16} Nonbonding interactions have also been utilized in biasing the conformations of flexible molecules.^{17,18} These conformationally biased flexible molecules may be more likely to find low energy conformations in complexation processes without significant enthalpic penalty over rigid systems through *dynamic complementarity*.¹⁹

The Bcl-2 family of proteins is the key regulator of programmed cell death.²⁰ Bcl-2 family members contain from one to four Bcl-2 homology (BH) domains and can be broadly divided into two classes; anti-apoptotic and pro-apoptotic

[†] Cancer Research.

[‡] Advanced Technologies.

- (1) Galeazzi, R.; Mobbili, G.; Orena, M. *Curr. Org. Chem.* **2004**, *8*, 1799–1829.
- (2) Bartlett, P. A.; Yusuff, N.; Pyun, H.-J.; Rico, A. C.; Meyer, J. H.; Smith, W. W.; Burger, M. T. *Spec. Publ.-R. Soc. Chem.* **2001**, *264*, 3–15.
- (3) Hruby, V. J. *Acc. Chem. Res.* **2001**, *34*, 389–397.
- (4) Houk, K. N.; Leach, A. G.; Kim, S. P.; Zhang, X. *Angew. Chem., Int. Ed.* **2003**, *42*, 4872–4897.
- (5) Cram, D. J. *Angew. Chem., Int. Ed. Engl.* **1986**, *25*, 1039–1134.
- (6) Ciani, B.; Jourdan, M.; Searle, M. S. *J. Am. Chem. Soc.* **2003**, *125*, 9038–9047.
- (7) Ilioudis, C. A.; Tocher, D. A.; Steed, J. W. *J. Am. Chem. Soc.* **2004**, *126*, 12395–12402.
- (8) Reichelt, A.; Gaul, C.; Frey, R. R.; Kennedy, A.; Martin, S. F. *J. Org. Chem.* **2002**, *67*, 4062–4075.
- (9) Meyer, J. H.; Bartlett, P. A. *J. Am. Chem. Soc.* **1998**, *120*, 4600–4609.

- (10) Barboni, L.; Lambertucci, C.; Appendino, G.; Vander Velde, D. G.; Himes, R. H.; Bombardelli, E.; Wang, M.; Snyder, J. P. *J. Med. Chem.* **2001**, *44*, 1576–1587.
- (11) Bartlett, S.; Beddard, G. S.; Jackson, R. M.; Kayser, V.; Kilner, C.; Leach, A.; Nelson, A.; Oledzki, P. R.; Parker, P.; Reid, G. D.; Warriner, S. L. *J. Am. Chem. Soc.* **2005**, *127*, 11699–11708.
- (12) Dinsmore, C. J.; Bogusky, M. J.; Culberson, J. C.; Bergman, J. M.; Homnick, C. F.; Zartman, C. B.; Mosser, S. D.; Schaber, M. D.; Robinson, R. G.; Koblan, K. S.; Huber, H. E.; Graham, S. L.; Hartman, G. D.; Huff, J. R.; Williams, T. M. *J. Am. Chem. Soc.* **2001**, *123*, 2107–2108.
- (13) Hanessian, S.; Moitessier, N. *Curr. Top. Med. Chem.* **2004**, *4*, 1269–1287.
- (14) Babine, R. E.; Bender, S. L. *Chem. Rev.* **1997**, *97*, 1359.
- (15) Wacowich-Sgarbi, S. A.; Bundle, D. R. *J. Org. Chem.* **1999**, *64*, 9080–9089.
- (16) Davidson, J. P.; Lubman, O.; Rose, T.; Waksman, G.; Martin, S. F. *J. Am. Chem. Soc.* **2002**, *124*, 205–215.
- (17) Knust, H.; Hoffmann, R. W. *Chem. Rec.* **2002**, *2*, 405–418.
- (18) Hodge, C. N.; Lam, P. Y. S.; Eyerhmann, C. J.; Jadhav, P. K.; Ru, Y.; Fernandez, C. H.; De Lucca, G. V.; Chang, C.-H.; Kaltenbach, R. F., III; Holler, E. R.; Woerner, F.; Daneker, W. F.; Emmett, G.; Calabrese, J. C.; Aldrich, P. E. *J. Am. Chem. Soc.* **1998**, *120*, 4570–4581.
- (19) Morgan, B. P.; Holland, D. R.; Matthews, B. W.; Bartlett, P. A. *J. Am. Chem. Soc.* **1994**, *116*, 3251–3260.
- (20) Danial, N. N.; Korsmeyer, S. J. *Cell* **2004**, *116*, 205–219.

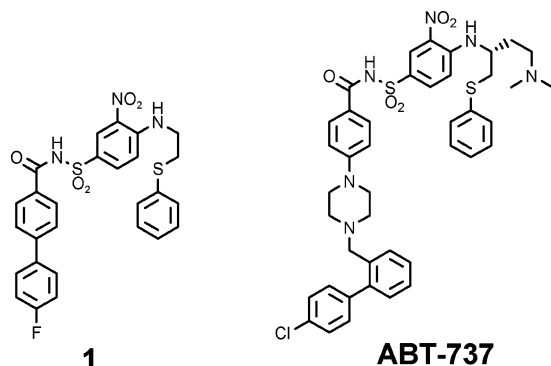


Figure 1. Chemical structures of inhibitors of Bcl-X_L **1** and ABT-737.

proteins. The anti-apoptotic proteins (e.g., Bcl-2, Bcl-X_L) are characterized by four BH domains, BH1–4. The pro-apoptotic proteins can be further subdivided into those that incorporate three BH domains (e.g., Bax, Bak) and the BH3-only proteins (e.g., Bad, Bid, Bim, Bik). The interplay between these three groups of proteins serves as the gateway to the intrinsic apoptosis pathway.^{21–24} Under conditions of cellular stress, pro-apoptotic BH3-only proteins (e.g., Bid, Bim) are mobilized to activate the direct mediators of apoptosis, Bax and Bak. Upon activation, cytochrome C release from the mitochondria leads to formation of the apoptosome which initiates the caspase-9 pathway. The anti-apoptotic proteins, Bcl-2 and Bcl-X_L, prevent this activation by directly binding to and sequestering these pro-apoptotic proteins. Due to the overexpression of Bcl-2 and Bcl-X_L in numerous types of tumors, compounds selectively inhibiting Bcl-2 and Bcl-X_L would be of great therapeutic value for cancer. A number of approaches have been reported in the literature, including peptide conjugates, natural products, virtual screening, high-throughput screening, and structure-based design.²⁵

We have recently reported the discovery of the potent Bcl-X_L ligand **1** by an NMR-based fragment screening technique (SAR by NMR) and structure-guided parallel synthesis.²⁶ Further elaboration of **1** led to the discovery of ABT-737, which displayed subnanomolar binding affinities to Bcl-2, Bcl-X_L, and Bcl-w, which regressed established tumors in murine xenograft models.^{27,28} Figure 1 shows the chemical structures of inhibitors of Bcl-X_L **1** and ABT-737; Figure 2 shows a schematic diagram of critical binding interactions between compound **1** and Bcl-X_L.²⁶ Intramolecular π -stacking interactions between the nitrophenyl and thiophenyl groups of **1** induce a folded conformation that fits nicely into the binding pocket formed by BH1 and BH3 domains of the protein. Furthermore, these two aromatic rings engage in intermolecular interactions with the aromatic groups of the surrounding protein residues: (a) the nitrophenyl group with Tyr194 in “herring bone” structure (intersection angle of about 45° between the two planes of rings) and (b) the thiophenyl group with Phe97 in a parallel-displaced structure and with Tyr101 in a displaced T-shape (intersection angle of about 90° between the two planes of rings). This extensive intra-

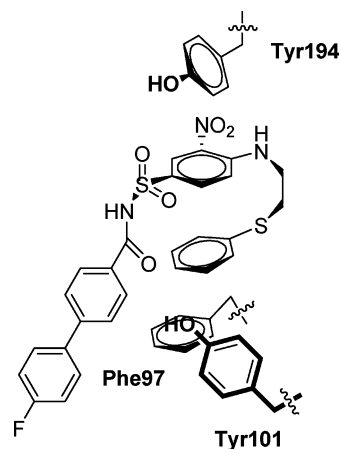


Figure 2. Schematic diagram of an NMR-based structure of compound **1** bound to Bcl-X_L showing the key residues lining the binding site.

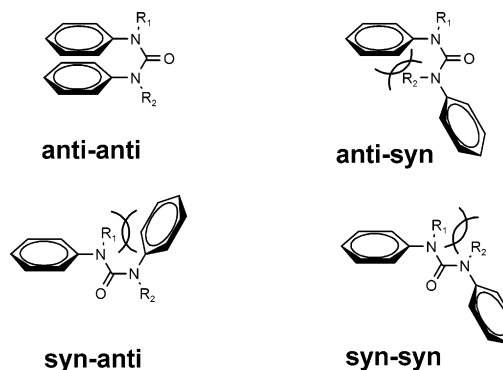


Figure 3. Four representative conformations of *N,N'*-diarylurea.

and intermolecular π – π interaction network is essential for tight binding to this large surface area, hydrophobic binding site and serves as one of the key anchoring points for the ligand.

Given the significant contribution to binding affinity from this π – π interaction network created by the folded conformation, we were prompted to explore alternative tethers that might bias the molecule to adopt this conformation by utilizing nonbonding interactions. We chose to explore *N,N'*-diarylureas due to their unique preference to adopt folded conformations.²⁹ The four possible *N,N'*-diarylurea conformations are shown in Figure 3 and are defined on the basis of the orientation of the aryl groups relative to the urea carbonyl group. To examine whether a urea tether would preorganize the compound to adopt an appropriate folded conformation, compounds **2**, **3**, and **4** containing systematic alterations in nitrogen substitution were prepared. Their binding affinities were compared with that of the parent bent-back compound **18**, and the conformational preferences and flexibilities were further analyzed using X-ray crystallography, quantum mechanical calculations, and NMR spectroscopy.

Results and Discussion

Design and Synthesis. The three closely related compounds **2**, **3**, and **4** shown in Figure 4 were chosen to probe the effect of nonbonding interactions arising from simple nitrogen substitution on overall *N,N'*-diarylurea conformation. Figure 5 shows atom and torsional angle numbering. We reasoned that

(21) Cory, S.; Adams, J. M. *Nat. Rev. Cancer* **2002**, *2*, 647–656.

(22) Hanahan, D.; Weinberg, R. A. *Cell* **2000**, *100*, 57–70.

(23) Borner, C. *Mol. Immunol.* **2003**, *39*, 615–647.

(24) van Delft, M. F.; Huang, D. C. S. *Cell Res.* **2006**, *16*, 203–213.

(25) Elmore, S. W.; Oost, T. K.; Park, C.-M. *Annu. Rep. Med. Chem.* **2005**, *40*, 245.

(26) Petros, A. M.; et al. *J. Med. Chem.* **2006**, *49*, 656–663.

(27) Oltersdorf, T.; et al. *Nature* **2005**, *435*, 677–681.

(28) Wendt, M. D.; et al. *J. Med. Chem.* **2006**, *49*, 1165–1181.

(29) Kurth, T. L.; Lewis, F. D.; Hattan, C. M.; Reiter, R. C.; Stevenson, C. D. *J. Am. Chem. Soc.* **2003**, *125*, 1460–1461 and references therein.

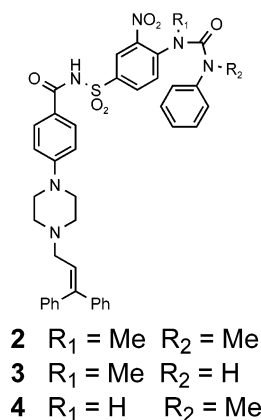


Figure 4. Compounds containing N,N' -diarylurea motifs.

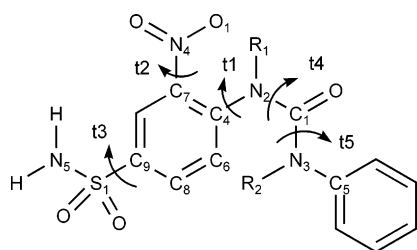


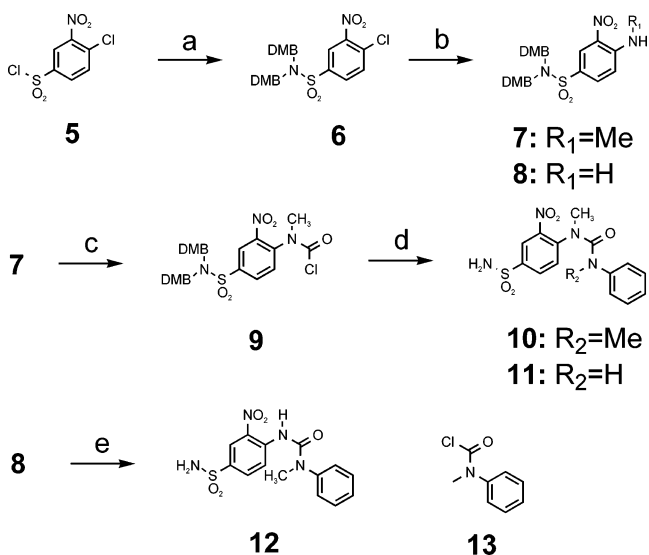
Figure 5. Atom and torsional angle numbering.

the desired anti–anti folded conformation would be most favored by the disubstitution found in **2** because of (a) the presence of reinforcing π -stacking interaction between the aromatic groups in **2** and (b) the presence of unfavorable steric interactions between methyl aryl or methyl alkyl groups in the anti–syn, syn–anti, and syn–syn conformers (Figure 3). Compounds **3** and **4**, both of which contain a single nitrogen methyl group, would have less potential for such steric interactions. We sought to explore how modifications of the urea substitution pattern influenced the energetic preference for conformation and the binding affinity to Bcl-X_L.

The synthesis of compound **2** commenced with the preparation of sulfonamide **6** by coupling of the sulfonyl chloride **5** with bis-2,4-dimethoxybenzylamine (Scheme 1). Nucleophilic aromatic substitution of chloride **6** with methylamine gave aniline **7**, which was treated with phosgene to afford carbamoyl chloride **9**. Reaction of **9** with *N*-methylaniline, followed by deprotection with trifluoroacetic acid, yielded compound **10**. Carboxylic acid **16** was prepared by reductive amination of piperazine **14** with β -phenylcinnamaldehyde followed by saponification (Scheme 2). Carbodiimide-mediated coupling of sulfonamide **10** with carboxylic acid **16** yielded compound **2**. Compound **3** was prepared in a manner similar to compound **2** by reacting carbamoyl chloride **9** with aniline and the resulting urea **11** processed as above. Compound **4** was prepared by the reaction of aryl chloride **6** with ammonia and the resulting aniline condensed with carbamoyl chloride **13**.³⁰ Removal of the dimethoxybenzyl groups under acidic conditions and coupling of the resulting sulfonamide **12** with carboxylic acid **16** yielded compound **4**. Compound **18** was prepared by carbodiimide-mediated coupling of carboxylic acid **16** and sulfonamide **17**.²⁶

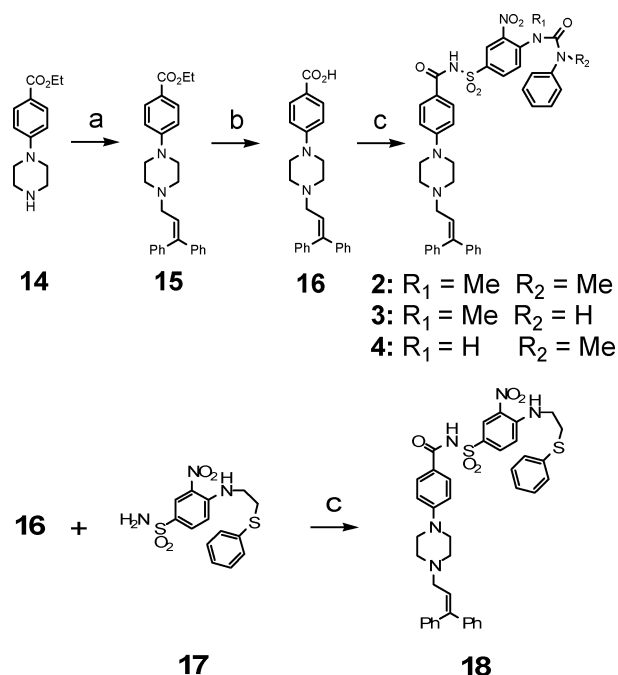
Binding Study. The binding constants for compounds **2**, **3**, **4**, and **18** to Bcl-X_L were determined using a fluorescence

Scheme 1^a



^a Reagents and conditions: (a) (DMB)₂NH, TEA, dichloromethane, 0 °C to room temperature (rt), 2 h; (b) for $R_1 = \text{Me}/\text{MeNH}_2$, MeOH/THF (3.5:1), 80 °C, overnight, sealed tube; for $R_1 = \text{H}/\text{NH}_3$, MeOH, 125 °C, 16 h, 120 PSI; (c) phosgene, PS-DIEA, dichloromethane/toluene, 50 °C, 24 h, sealed tube; (d) (i) for $R_2 = \text{Me}/\text{PhNH}(\text{Me})$, dichloromethane, rt, overnight; for $R_2 = \text{H}/\text{PhNH}_2$, dichloromethane, rt, overnight; (ii) dichloromethane/TFA/triethylsilane (1:0.9:0.1), rt, 2 h; (e) (i) **13**, DMAP, DIPEA, 1,2-dichloroethane, 80 °C, 36 h; (ii) dichloromethane/TFA/triethylsilane (1:0.9:0.1), rt, 2 h. DMB = 2,4-dimethoxybenzyl.

Scheme 2^a



^a Reagents and conditions: (a) (Ph)₂C=CHCHO, Na(OAc)₃BH, 1,2-dichloroethane, rt, overnight; (b) LiOH, THF/MeOH/H₂O (2:1:1), rt; (c) EDCI, DMAP, dichloromethane, rt, overnight, **10**, **11**, **12** for **2**, **3**, and **4**, respectively.

polarization assay as described previously.²⁶ Compounds **2** and **3** exhibited binding affinities of 5.0 and 7.4 nM, respectively, which is comparable to that of the parent compound **18** (1.1 nM) (Table 1). However, compound **4**, where $R_1 = \text{H}$, shows a significant loss of affinity (550 nM). These results prompted a more in-depth conformational analysis.

(30) Freer, R.; McKillop, A. *Synth. Commun.* **1996**, *26*, 331–350.

Table 1. Binding Affinity of the Compounds

compd	K_i (nM) ^a
18	1.1 ± 0.4
2	5.0 ± 0.8
3	7.4 ± 2.3
4	550 ± 170

^a The K_i values represent the mean ± SEM (n ≥ 3).

X-ray Crystallography. To examine the conformational preference of these compounds, we first focused our effort on determining the X-ray crystal structures of the fully elaborated compounds **2–4**. However, difficulties in obtaining suitable crystals of these molecules led us to examine the structures of the sulfonamide fragments **10**, **11**, and **12** as suitable surrogates. High-resolution single-crystal X-ray diffraction data were successfully obtained for **10** and **11**, but the data for **12** were of lower quality due to small crystal size. Consequently, the structure of **12** was independently determined using structure determination from powder diffraction (SDPD) techniques.³¹ The unit cell from the single-crystal data was fit to the experimental powder data using Pawly refinement to extract intensities. The starting model was based on the single-crystal structure, but all of the rotatable bonds and the orientation of molecules in the unit cell were perturbed. In the SDPD determination, all nonrigid bonds were allowed to rotate freely. The resulting structure was very similar in conformation to the single-crystal structure. The average root-mean-square deviation between equivalent atoms in the two models was 0.272 Å, with the greatest difference occurring in one of the two sulfonamide oxygen atoms.

The three crystal structures thus obtained are shown in Figure 6 and reveal that the relative orientations of the two phenyl groups with respect to the carbonyl group are all unique (anti–anti, syn–syn, and syn–anti, for compounds **10**, **11**, and **12**, respectively). Compound **10** displays the desired folded conformation in the crystal structure. The comparable Bcl-X_L binding affinity of compound **2** compared to that of compound **18** suggests the crystal structure may represent its protein-bound conformation. However, both sulfonamides **11** and **12** exhibit extended conformations in the crystal structure. This extended conformation is not consistent with the high binding affinity of **3**.

X-ray crystal structures may not necessarily represent the low energy conformations of flexible molecules due to the potentially significant contributions from intermolecular interactions involving adjacent and solvent molecules that are inevitable in the condensed states.³² In particular, the difference in conformations found in these compounds may be attributed in part to the difference in intermolecular hydrogen-bonding patterns. For example, the crystal structure of compound **10** reveals that its sulfonamide group is engaged in only one intermolecular hydrogen bond interaction (hydrogen bonds are represented as dotted lines in crystal packing lattice, Figure 6B). Compound **11**, on the other hand, has a much more extensive intermolecular hydrogen-bonding network involving both the sulfonamide and urea subunits that likely influences the preference for an extended conformation in the solid state. In addition to these

intermolecular hydrogen bonds, compound **12** also contains an intramolecular hydrogen bond between the aryl nitro group and the adjacent urea N–H that might provide a barrier to adopting a folded conformation. This is consistent with the dramatically lower binding affinity of **4**. The inconsistency between the conformation of **11** found in its crystal structure and the high binding affinity of **3** may suggest a small energy difference between the various conformations. To better examine this, we next determined global energy minimum conformations for **10–12** employing quantum mechanical calculations.

Quantum Mechanical Calculations. To assess the relative stability of the conformations of sulfonamides **10**, **11**, and **12**, quantum mechanical calculations were conducted.³³ Figure 8 illustrates the low energy conformations of the anti–anti (A1), anti–syn (B1), syn–syn (C1), and syn–anti (D1) forms for compounds **10**, **11**, and **12**. In addition, fragment **19** of the parent compound **18** containing the NHCH₂CH₂S linker was subjected to calculations, and the structures were compared with that found in complex with the protein (Figure 7).

For fragment **19** representing the parent compound **18**, the relative energies of the folded and extended conformers are of particular interest. The input geometries for the optimization of these two conformers were taken directly from the experimental NMR structure, but one torsional angle of N–C–S was adjusted to 180° in the input geometry of the extended conformer. The folded conformation **19A1** is more stable than the extended conformation **19B1** by 1.69 kcal/mol and exhibits conformation very similar to that found in the bound state (Figure 7).

The lowest energy conformation for **10** identified in these calculations (**10A1**, Figure 8A) matches very closely that found in the crystal structure except for the orientation of the sulfonamide group. The conformation (**10A2**, Figure 9) corresponding to the crystal structure (**10Xr**) is only 0.12 kcal/mol higher in energy than **10A1**. The conformations found in **10B1–10D1** are energetically disfavored (5.65–7.16 kcal/mol) likely due to the unfavorable methyl–methyl and methyl–phenyl steric interactions. It is not apparent from these studies the extent to which other intramolecular forces, such as π -stacking interactions, contribute to the folded conformation.

Calculations on compound **11** that lacks the N3 methyl group reveal that the folded conformation is still favored by 2.69–4.57 kcal/mol even in the absence of significant steric bias (Figure 8B, **11A–11D**). This may explain the nearly identical potency of **3** in comparison to that of **2**. The next higher energy conformation **11B1** (2.69 kcal/mol) differs only in the orientation of the terminal aryl group and underscores the propensity to form π -stacking interactions^{34,35} even at the expense of partial loss of conjugation between N3 and the phenyl ring in **11A1**. It is noteworthy that the calculated energy of the conformation corresponding to the crystal structure (**11C2**, Supporting Information) is 4.58 kcal/mol higher than that of the global energy minimum conformation (**11A1**). This highlights the extent to which the intermolecular interactions inherent to the crystal lattice can bias conformational preference in the solid state.

The lowest energy conformation of **12** (**12D1**) found by calculations is in good agreement with that found in the crystal

(31) *MS Modeling, Powder Solve Module*, version 3.2; Accelrys Software: San Diego, CA, 2004.

(32) Dunitz, J. D.; Gavezzotti, A. *Acc. Chem. Res.* **1999**, *32*, 677–684.

(33) Details are provided in the Supporting Information.

(34) Rashkin, M. J.; Waters, M. L. *J. Am. Chem. Soc.* **2002**, *124*, 1860–1861.

(35) Tsuzuki, S.; Honda, K.; Uchimaru, T.; Mikami, M.; Tanabe, K. *J. Am. Chem. Soc.* **2002**, *124*, 104–112.

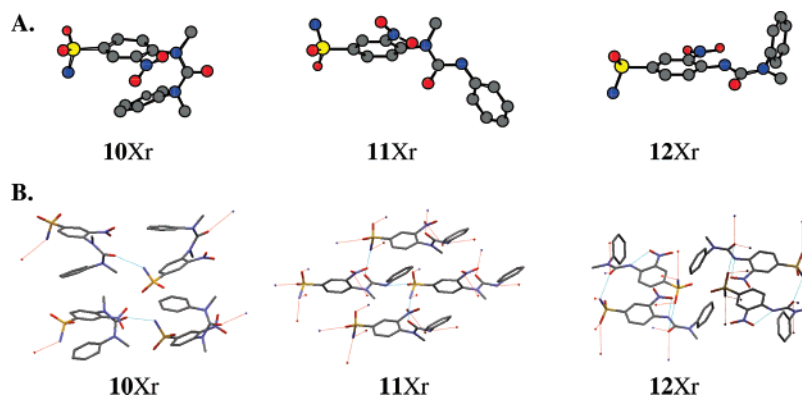


Figure 6. (A) Chem3D representations of the crystal structures. (B) Views of crystal packing generated by Mercury for **10**, **11**, and **12**. Hydrogen atoms are omitted for clarity.

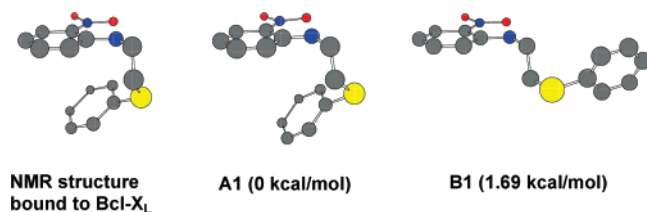


Figure 7. Comparison of the NMR structure for the fragment **19** of the parent compound **18** containing $\text{NHCH}_2\text{CH}_2\text{S}$ linker bound to Bcl-X_L with low energy conformations found by calculations.

structure (**12Xr**) (Figure 8C). This conformation provides maximal overlap of the π -systems of the nitro and urea nitrogens and carbonyl group. This extended conjugation contributes to the energetic differences between **12D1** and the other potential conformers (4.10–10.81 kcal/mol). Compound **12**, which lacks the N2 methyl group, displays features drastically different from those of compound **11** in that the proton on N2 is poised to form an intramolecular hydrogen bond (1.812 Å between hydrogen and oxygen atoms in the calculated structure) with the oxygen atom of the nitro group. The most accessible folded conformation of **12** (**12A1**) is significantly higher in energy (5.15 kcal/mol) than the global minimum (**12D1**), rendering it much less available as a bioactive conformation. This presumably explains why the binding affinity of **4** is reduced by more than 2 orders of magnitude relative to that of either **2** or **3**, which are easily able to adopt, and in fact prefer, the folded motif.

The two other extended conformations **12B1** and **12C1** are 9.16 and 4.10 kcal/mol higher in energy than the global minimum, respectively. The significantly higher energy of **12B1** in comparison to **12C1** appears, at least in part, to be due to a loss of conjugation of the π -system involving N2–C1 (torsional angle τ of 61.6° in comparison to –176.7° in **12C1**). Although the origin of the large energy difference (4.10 kcal/mol) between **12C1** and **12D1** is not immediately apparent, it might be rationalized by considering a potentially stabilizing electrostatic interaction between the electron-deficient proton on N2 and the π -electrons of the phenyl group on N3 (the distance of 2.31 Å between hydrogen atom and phenyl ring) in **12D1**.^{36,37}

The hydrogen bonds between the nitro group and the proton on N2 found in all of the local energy minimum structures of **12** prompted us to investigate the contribution of this type of

hydrogen bond to the stabilization of the structures.³⁸ The geometries devoid of this hydrogen bond (**12A2–D2**) were generated by rotating the nitrophenyl ring of **12A1–D1** by 180° followed by energy minimization, and the resulting conformations were compared to those containing the hydrogen bond (Figure 8D). The energy differences for **12A1–12A2** and **12B1–12B2**, 0.58 and 1.65 kcal/mol, respectively, are significantly smaller than those for **12C1–12C2** and **12D1–12D2**, 4.49 and 3.91 kcal/mol, respectively. These apparently diminished contributions of the hydrogen bond in **12A1** and **12B1** can be attributed to the increased repulsive interaction between the oxygen atoms of carbonyl and nitro groups (respective O···O distances of 4.275 and 4.334 Å in **12A1** and **12B1** versus 4.923 and 4.941 Å in **12C1** and **12D1**). Additional contribution to the stability of **12C1** and **12D1** can be identified in the attractive electrostatic interaction between the aromatic hydrogen atom at C6 and the carbonyl oxygen atom (H···O distances of 2.089 and 2.080 Å, respectively).^{39,40}

Thus, the local conformation around the nitro group appears to be one of the key factors in governing the overall conformation (folded versus extended). The methyl groups on N2 in compounds **10** and **11** steer the nitrophenyl ring out of amide bond conjugation, leading to a folded conformation being favored over the extended. The presence of the additional N3 methyl group in **10** enhances the preference for the folded conformation compared to **11** (5.65 versus 2.72 kcal/mol difference from the lowest energy extended conformation) due to unfavorable steric interactions in the alternative conformers. On the other hand, compound **12**, which lacks the N2 methyl, is able to engage in an intramolecular hydrogen bond that allows a high degree of π -conjugation that highly favors an extended conformation.

Solution Structure of the Protein–Ligand Complex. These studies suggest that compounds such as **2** containing N,N'-disubstituted diarylurea would prefer a folded conformation and easily adopt the putative bioactive conformation. To confirm this, we obtained a solution structure of compound **2** bound to Bcl-X_L .

All structure calculations were carried out with the program CNX.⁴¹ Initially, compound **2** was randomly positioned near

(36) Rashkin, M. J.; Hughes, R. M.; Calloway, N. T.; Waters, M. L. *J. Am. Chem. Soc.* **2004**, *126*, 13320–13325.

(37) Lavieri, S.; Zoltewicz, J. A. *J. Org. Chem.* **2001**, *66*, 7227–7230.

(38) Allen, F. H.; Baalham, C. A.; Lommerse, J. P. M.; Raithby, P. R.; Sparr, E. *Acta Crystallogr., Sect. B* **1997**, *53*, 1017–1024.

(39) Pierce, A. C.; terHaar, E.; Binch, H. M.; Kay, D. P.; Patel, S. R.; Li, P. *J. Med. Chem.* **2005**, *48*, 1278–1281.

(40) Taylor, R.; Kennard, O. *J. Am. Chem. Soc.* **1982**, *104*, 5063–5070.

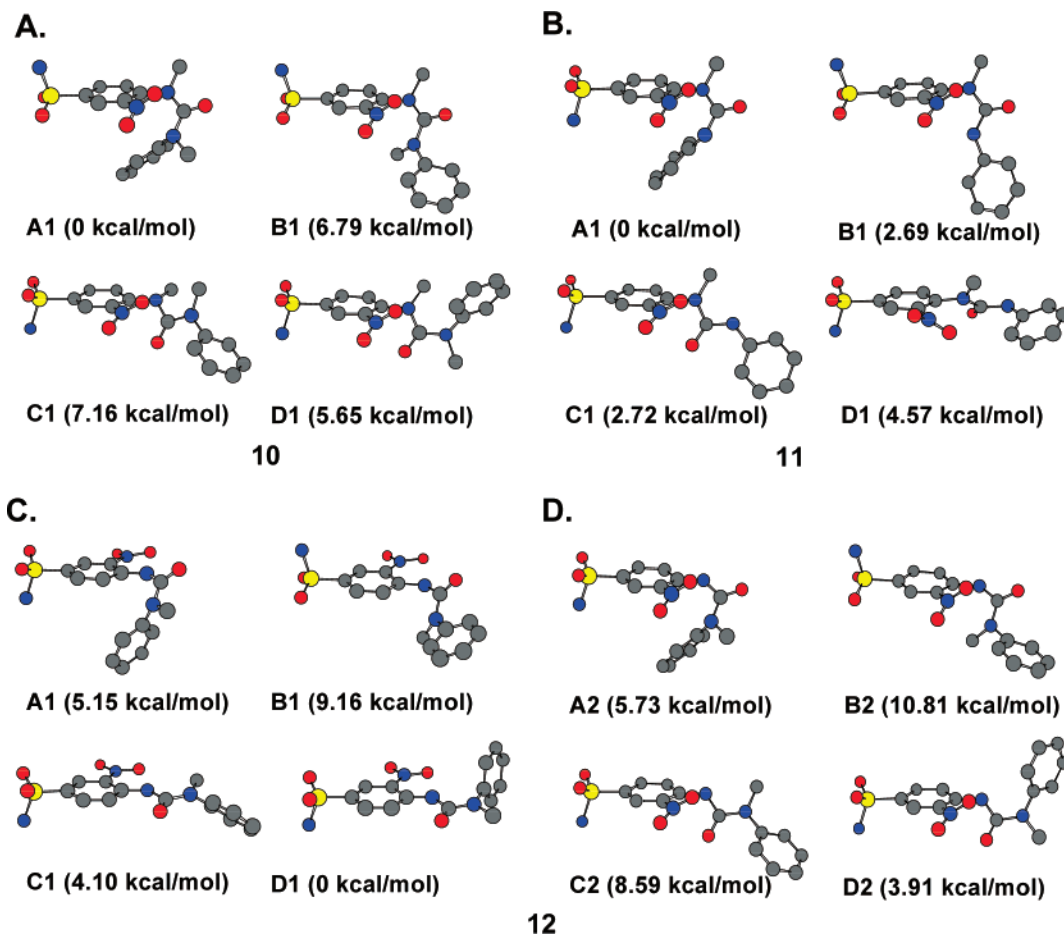


Figure 8. Low energy conformations of the anti–anti (A1), anti–syn (B1), syn–syn (C1), and syn–anti (D1) forms for compounds **10**, **11**, and **12** (A, B, and C, respectively) and conformations for compound **12** lacking hydrogen bonding (D).⁴⁴

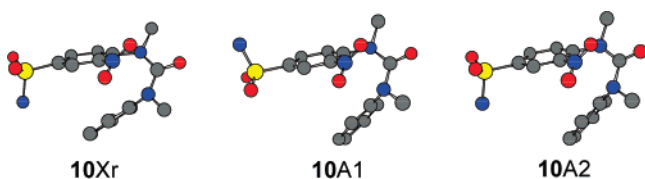


Figure 9. Comparison of the crystal structure (**10Xr**) and the two lowest energy structures (**10A1**, **10A2**).

the binding groove of Bcl-X_L and the observed intermolecular NOEs were used to dock the ligand into the groove. This docking was followed by energy minimization and a standard simulated annealing protocol.⁴² During the simulated annealing, the coordinates of the protein were held fixed, with the exception of those residues that line the binding groove (residues 96–112, 127–142, and 191–194). This protocol was based on the structural studies of Bak peptide binding to Bcl-X_L, for which we observed structural rearrangements only for residues lining the hydrophobic groove upon peptide binding.⁴³ The conformation of these residues was governed by the observed intermo-

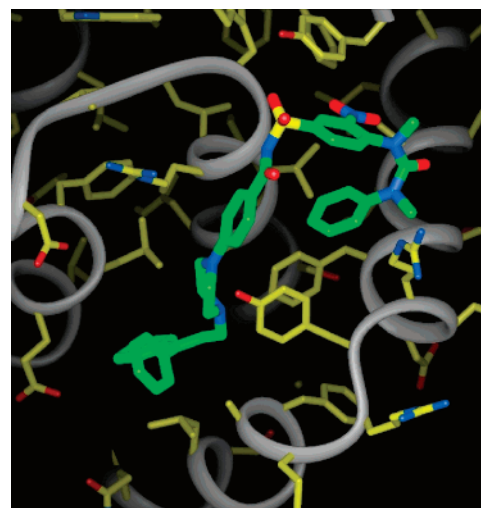


Figure 10. NMR-based solution structure of compound **2** bound to Bcl-X_L.

lecular NOEs. For compound **2**, a total of 100 intermolecular NOEs were used to dock the ligand to Bcl-X_L.

Figure 10 shows the solution structure of **2** bound to the protein. Indeed, the urea moiety of compound **2** exhibits a folded conformation and a very similar arrangement of the π -interaction network found in compound **1** complexed with the protein (Figure 2); the nitrophenyl group on N2 with Tyr194, the phenyl group on N3 with Phe97 and Tyr101. These results unequivocally

(41) Brunger, A. T. *X-PLOR*, version 3.1; Yale University Press: New Haven, CT, 1992.

(42) Kuszewski, J.; Nilges, M.; Brunger, A. T. *J. Biomol. NMR* **1992**, *2*, 33–56.

(43) Sattler, M.; Liang, H.; Nettlesheim, D.; Meadows, R. P.; Harlan, J. E.; Eberstadt, M.; Yoon, H. S.; Shuker, S. B.; Chang, B. S.; Minn, A. J.; Thompson, C. B.; Fesik, S. W. *Science* **1997**, *275*, 983–986.

(44) The Cartesian coordinates along with torsional angles and energies of all minimized geometries are provided in the Supporting Information.

cally establish the bioactive conformation of the urea motif of compound **2** being a folded conformer.

To gain an idea on the bound conformation of the urea in compound **3**, we briefly investigated the compound in the presence of Bcl-X_L by NMR. The similarity of the NOE pattern in conjunction with the results from binding, crystallography, and calculations led us to conclude that the folded conformation of the urea group in compound **3** also represents its bound conformation. The intermediate exchange rate of compound **4** for Bcl-X_L prohibited us from obtaining high quality spectra. However, the weak binding affinity of **4** is consistent with the diminished population of the bioactive conformation due to the high energy of the folded conformation of the urea motif.

Conclusions

The concept of preorganization has been widely utilized in the area of molecular recognition, including small molecule–protein interactions. The binding affinity of a ligand for a protein could be improved with higher complementarity between a ligand and a receptor binding site. The folded conformation found in inhibitors bound to Bcl-2 family proteins led us to design compounds with alternative motifs to favor the protein-bound conformation. To circumvent some of the pitfalls associated with constraining a conformation by covalent modifications, we have instead exploited nonbonding interactions. Evaluation of structurally related analogues using target protein binding affinity, X-ray crystallography, and quantum mechanical calculations allowed us to gain insight into factors influencing the bioactive conformations of a series of differentially substi-

tuted ureas **2**, **3**, and **4**. While **2** and **3** (corresponding to sulfonamide **10** and **11**, respectively) bind to the protein with high affinity (5.0 and 7.4 nM), **4** (corresponding to sulfonamide **12**) shows a dramatic loss of potency (550 nM). The high affinity of **2** and **3** can be explained by the heavy population of the global energy minimum conformers that adopt folded conformations of the urea subunits. The folded conformations **10A1** and **11A1** are separated from the next higher energy conformations **10D1** and **11B1** by 5.65 and 2.69 kcal/mol, respectively. The significantly lower binding affinity of **4** arises from the large preference (5.15 kcal/mol) for a highly conjugated, extended urea conformation (**12D1**) that is due, at least in part, to the presence of an intramolecular hydrogen bond. The folded conformation of **2** that was predicted by both the X-ray crystal structure studies and energy minimization calculations on the sulfonamide surrogate **10** to be favored was indeed found to be its protein-bound conformation by obtaining the NMR solution structure of **2** bound to Bcl-X_L.

Acknowledgment. We thank Thomas B. Borhardt for the powder X-ray study and the staff of Structural Chemistry and Pressure Lab for NMR, MS, and high-pressure reactions.

Supporting Information Available: Experimental details, X-ray crystallographic data for **10**, **11**, and **12** in CIF format, Cartesian coordinates and energies of structures **10**, **11**, **12**, and **19**, and complete citation for refs 26–28. This material is available free of charge via the Internet at <http://pubs.acs.org>.

JA0650347